16TH EUROPEAN CONFERENCE ON EARTHQUAKE ENGINEERING THESSALONIKI 18 - 21 JUNE 2018

LOCAL EFFECTS DUE TO AAC MASONRY INFILL - RC FRAME INTERACTION THROUGH SIMULATION OF IN-PLANE TESTS WITH FEM ANALYSES

Riccardo R. MILANESI[1], Paolo MORANDI[2], Guido MAGENES[3]

ABSTRACT

The seismic design of unreinforced masonry infills, which are widely used in many parts of the world, commonly uses simplified methods that usually do not consider the interaction between the infill and the structure. The scientific interest on masonry infills is continuously raising in the last decades due to the unsatisfactory seismic response of the infilled frame structures observed during post-event inspections and the difficulty to contrive a solution which is widely scientifically and practical recognized. Although some modern codes consider the presence of infills with some prescriptions to prevent damage in the masonry panels and to take into account global and local effects on the structure due the presence of the infills, an effective evaluation of these detrimental effects has not been achieved yet. Within this paper, the main results of a numerical campaign of a RC frame specimens with Autoclaved Aerated Concrete (AAC) masonry infill are presented in order to study accurately the influence and the interaction of the infill with the RC structure. The in-plane pseudo-static cyclic experimental results of the tests performed by Calvi and Bolognini (1999), and Penna and Calvi (2006) on one-bay one-storey full-scale specimens are taken as reference and simulated. FEM non-linear static analyses using a "meso-modelling" approach have been carried out. The masonry used in the model has been calibrated according to tests of mechanical characterization as discussed by Milanesi et al. (2015). The analyses performed have allowed to investigate the local effects on the frame and a comparison between the actual moment and shear demands on the RC elements due to the presence of the AAC infill and the ones in the bare structure is presented; moreover, the local pressure due to the infill along the contact length have been estimated depending by the drift imposed.

Keywords: local effects; infill-structure interaction; AAC masonry infill; FEM simulation; in-plane seismic response.

1. INTRODUCTION

Unreinforced masonry (URM) infills represent a widely used solution as non-structural panels in RC frame structures in many European countries. Although the current code provisions give few recommendations for these elements they revealed to be often unsuitable or not clearly defined for specific prevention of the damage and even of the human lives, as observed during post-event field inspections after major earthquakes (Manzini et al., 2012; Fragomeli et al., 2017).
Therefore, the scientific interest on the seismic behaviour of the infill is extremely active, and many researchers have conducted different investigations through experimental (Mehrabi, 1994; Calvi et al., 1999; Da Porto et al., 2012; Morandi et al., 2017) and numerical (Asteris et al., 2011; Tarque et al., 2015; Lourenço, 1995; Stavridis, 2009) studies.
The unsatisfactory seismic behaviour of the infills may be related both to intrinsic weakness of the traditional unreinforced masonry and to deficiencies in design criteria. Moreover, during the last

[1]Ph.D. Researcher, Department of Civil Engineering and Architecture, University of Pavia, Pavia, Italy, riccardo.milanesi@unipv.it
[2]Ph.D. Senior Researcher, Department of Civil Engineering and Architecture, University of Pavia and EUCENTRE Foundation, Pavia, Italy, paolo.morandi@unipv.it
[3]Full Professor, Department of Civil Engineering and Architecture, University of Pavia and EUCENTRE Foundation, Pavia, Italy, guido.magenes@unipv.it

lustrum, many studies of different innovative infills and possible improvements of the seismic performance are leading to the development of new products and innovative systems (i.e. Preti et al., 2012; Lin et al., 2016; Morandi et al., 2016; Verlato et al., 2016; Vintzileou et al., 2016).
In addition, the Autoclaved Aerated Concrete (AAC) masonry, which is gradually increasing its employment for both structural and non-structural purpose thanks to its lightness, excellent thermal and acoustic insulation and the fire resistance, has been barely studied in terms of seismic behaviour and will need to be adequately investigated through experimental and numerical researches.

(a)  (b) 

Figure 1. Masonry infill damage after Italian earthquakes: (a) Emilia earthquake in 2012 (Manzini et al., 2012); (b) Central Italy earthquake in 2016-2017 (Fragomeli et al., 2017).

In this paper, the FEM simulation of the in-plane pseudo-static cyclic tests on a RC frame specimen infilled with unreinforced AAC masonry infill tested by Penna and Calvi (2006) is presented; moreover, the investigation has been focused on the influence and the interaction of the infill with the RC structure. Non-linear static analyses using a "meso-modelling" approach have been carried out and the masonry constitutive law has been calibrated according to tests of mechanical characterization discussed in detail by Milanesi et al. (2015).
The results of the analyses have been interpreted in order to evaluate the local effects on the frame; the study has been focused on the distribution of moment and shear demands on RC elements due to the presence of the AAC infill respect to the bare frame. Finally, the local pressure acting on the RC column is discussed.

2. CURRENT EUROPEAN SEISMIC PROVISIONS FOR INFILLED STRUCTURES

According to the European code seismic provisions for infills, that are reported in Eurocode 8 (CEN, 2004), the structures located in seismic prone regions have to be designed and built respecting the life safety and damage limit states. Thus, in order to withstand the ultimate limit state (ULS), the structure have to maintain the structural integrity and a residual load bearing capacity after the seismic event, and local and global collapses have to be avoided. The design and construction of the structure to Damage Limit State (DLS) according to European seismic provisions is conducted in terms of displacement.
The damage limitation requirements, according to Eurocode 8 (EC8), are considered satisfied if the inter-storey drift $d_{r,DLS\,j} / h_j$ ($d_{r,DLS\,j}$ is the inter-storey displacement for storey j induced by the damage limitation seismic action, and h_j is the storey height) does not exceed the inter-storey limitation d_{DLS} which depends on the typology of non-structural element. Although the definition of the typologies is not clear and could be improved to avoid misinterpretations, the EC8 states that the inter-storey drift limitations for buildings are 0.50% for brittle non-structural elements attached to the structure, 0.75% for ductile non-structural elements, and 1.00% in case of absence of non-structural elements or with elements that do not interfere with the structure.
At the ULS, the safety verification, which has to be accomplished in terms of resistance to seismic action, effects for both structural and non-structural elements. In particular, for non-structural elements that might, in case of failure, threat the human life or affect the main structure of the building or services of critical facilities, as the infills, the verification is achieved by ensuring an out-of-plane resistance larger than the out-of-plane seismic force acting on the infill (usually defined as a horizontal out-of-plane force applied at the centre of mass of the infill). Moreover, the structural inter-storey drift

limitation is usually employed to avoid widespread damages within the infill.
The EC8 prescriptions for the local effects are referred to the critical length only; indeed, the critical length, which is defined in the RC design of each element depending by the ductility class, is increased, due to the presence of the infill, to the total height of the RC column only in specific cases which are: columns at the ground floor, infill in full contact with the column only on one side, and columns in partial contact with the infill (see Figure 2).

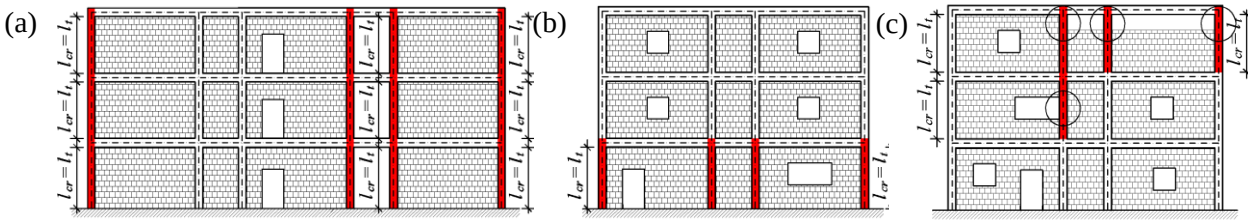

Figure 2. Critical length of the columns (a) in full contact with the infill on one side, (b) columns at the ground floor, and (c) columns in partial contact with the infill (Hak et al., 2013a).

3. FINITE ELEMENT MODEL: DESCRIPTION AND CALIBRATION OF THE MASONRY ACCORDING TO TESTS OF MECHANICAL CHARACTERIZATION

In the present section a general overview of the description of the FEM and of the calibration process of the materials is reported, more detailed information can be found in Milanesi et al. (2015).

3.1 Description of the FEM: general overview, geometry and elements typology, constitutive laws

The modelling of the RC members and the masonry infill has been achieved through a "meso-modelling" (Lourenço, 1995) with the aid of TNO Diana software (2010), where the materials are modelled as homogenous; thus, the masonry has not been defined through elements representing the mortar joints and the masonry units separately. The meso-model approach allows the calibration according to the test of characterization of the masonry, which is considered as a unique material without distinction between the unit and the mortar materials; indeed, the mechanical behaviour of the masonry is implicitly taken into account through a proper calibration of the masonry material (see *Section 3.2*).
The modelling of a masonry infill in a RC frame through finite element approaches may usually be subdivided into two well-known crack models: discrete and smeared (Roots, 1998), which can be further characterized into fixed and rotating smeared crack approaches. In the present work, the smeared total strain rotating crack model, originally proposed by Vecchio and Collins (1986), has been used for the concrete and the AAC masonry infill.
The RC frame and the masonry infill have been modelled with an eight-node quadrilateral iso-parametric plane stress element (Figure 3a) based on quadratic interpolation and Gauss integration with 4 integration points per elements. The frame-infill interface has been modelled using six-node interface elements (Figure 3b).

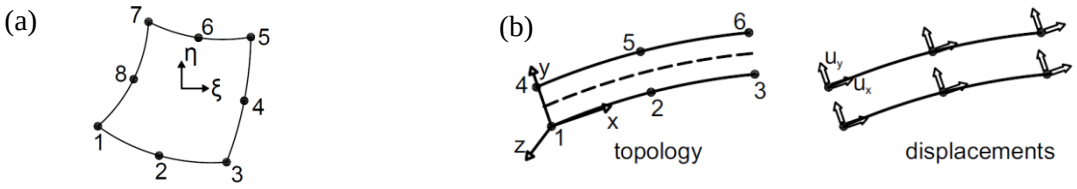

Figure 3. (a) 8-node quadrilateral iso-parametric plane stress element; (b) Frame-infill 6-node interface element.

The same constitutive model has been used for the concrete of the frame and for the AAC masonry infill. A parabolic behaviour under compression has been assumed for the concrete and the AAC masonry (Figure 4a) and the compressive strength, along with the compressive fracture energy, has been defined. The "crack bandwidth" *(h)*, which is contingent on the element size and the type of element used and,

in this particular case, it corresponds to the characteristic element length, has been computed automatically by the finite element software in order to avoid the "size effect". The reduction of the compressive strength due to lateral cracking has been considered according to the relationship proposed by Vecchio and Collins (1986) (Figure 4b). In addition, the increase of the compressive strength due to lateral confinement has been taken into account, using the model proposed by Selby and Vecchio (1993). The tensile behaviour has been idealized according to the model developed by Hordijk (1991) (Figure 4c). The tensile strength f_{ctm} has been computed with the formulae of Eurocode 2 (CEN, 2004), and the Mode-I fracture energy has been considered according to CEB-FIP Model Code 2010 (CEB-FIP, 2010). As an alternative, an elastic-brittle tensile constitutive model has also been used during the calibration of the material constitutive model used for the masonry. According to the elastic-brittle model the material has a perfect elastic tensile behaviour up to the maximum tensile stress (f_t), where the tensile resistance drops to zero.
For the reinforcing steel, the Von Mises yield criterion was adopted, with a bilinear stress-strain curve in uniaxial tension. The reinforcement steel bars have been considered as "embedded reinforcement" which add stiffness to the finite element model, as discussed by many authors (i.e Barzegar *et al.*, 1994 and Markou *et al.*, 2012). In this modelling technique, the reinforcing bars, which are explicitly modelled according to their real location and are not assumed as spread, are assumed to do not occupy any space or mass in the finite element model and the addition of embedded bars does not provide any weight to the mother element. The strains of the reinforcement are computed from the displacement field of the mother elements assuming perfect bond with the surrounding material.
The frame-infill interface elements employ a Coulomb Friction criterion (Figure 4d). The linear normal and tangential stiffness of the interface elements were assumed to be the same. The cohesion *c* and the friction coefficient *tanΦ* were computed from initial shear tests according to EN 1052-3 (2007). This model assumes that a gap forms if the tensile strength is exceeded.

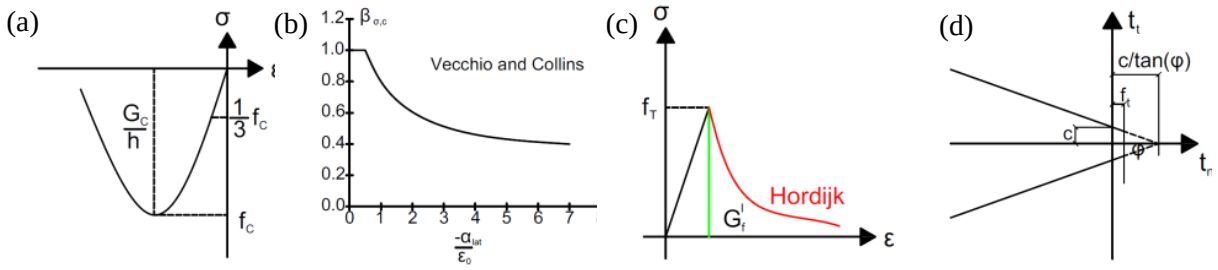

Figure 4. (a) Parabolic compressive behaviour which can be used in rotating crack model; (b) Vecchio and Collins relationship for reduction factor due to lateral cracking; (c) Hordijk tensile constitutive law which can be used in rotating crack model (red line); brittle tensile constitutive law (green line); (d) Coulomb friction criterion with tensile strength limit.

3.2 Calibration of the AAC masonry through simulation of the tests of characterization

Penna and Calvi (2006), during the experimental campaign, have performed a series of tests of characterization in order to know the mechanical behaviour of the AAC masonry adopted, which was composed by 30 cm thick AAC units and both head- and bed-joints with a thin layer of mortar (about 1 mm thick). In this work, the results of the vertical, horizontal and diagonal compressive strength tests have been considered and modelled.
The three vertical and the three horizontal compression tests on masonry wallettes, that have been conducted according to EN 1052-1 (2011), give a mean value of about 2.0 MPa in both direction; the seven specimens that have been subjected to the diagonal compression tests showed a shear strength (f_t) of 0.28 MPa ($f_t=0.5F_{max}/(t_w(b+l)/2)$, where F_{max} is the maximum applied load, t_w is the thickness of the masonry, and *b* and *l* are the dimensions of the specimen).
The masonry have been modelled with two different tensile behaviours (elastic-brittle and Hordijk) in order to compare the results and select the most suitable tensile constitutive law.
For both vertical and lateral compression, the stress-strain relations of the three cyclic tests are reported in Figure 5a and b, together with the results of the FEM pushover analyses (Figure 5a for the vertical

and Figure 5b for the horizontal compression). The results appear to be in good agreement, although the peak stress is not perfectly attained in both the cases (vertical and horizontal compression). The two laws used for modelling the tensile behaviour of the material have provided similar results in the case of the vertical compression tests but a different deformation capacity for the case of the horizontal compression test. For the diagonal compression tests, the comparison between the experimental and the numerical results with Hordijk and elastic-brittle tensile behaviour is shown in Figure 5c. The same parameters adopted for the vertical/horizontal compression tests are used. The Hordijk tensile behaviour presents a better accuracy in the descending branch, whereas the brittle model appears to predict slightly better the peak and its location in the load-displacement coordinates. In both cases, the stiffness and the obtained ultimate displacement have found to be accurate. The Hordijk tensile behaviour has been preferred to the elastic-brittle one because of better results of the descending branch in the post-peak region.

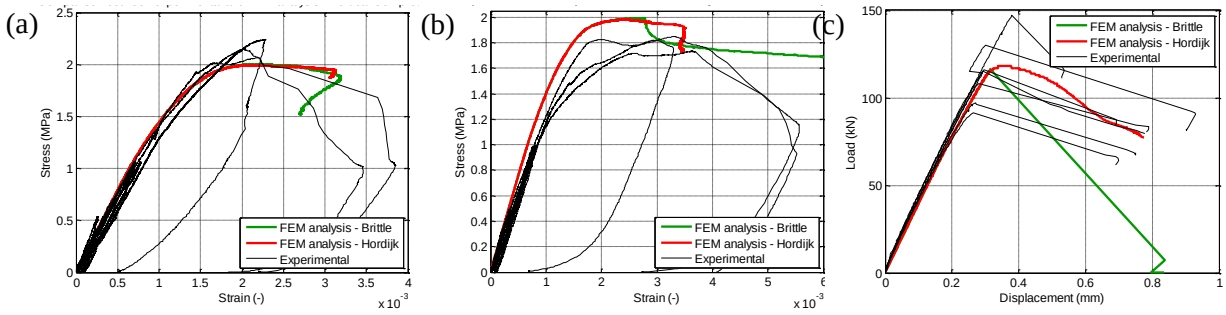

Figure 5. Comparison between experimental and FEM analysis: (a) vertical compression; (b) horizontal compression; (c) diagonal compression.

4. NUMERICAL SIMULATION OF THE IN-PLANE CYCLIC TESTS OF A RC BARE FRAME AND A RC FRAME INFILLED WITH AAC URM

The nonlinear static FEM analyses of a full-scale one-storey one-bay RC frame without infill and of a fully infilled RC frame with AAC URM have been performed.

4.1 Numerical simulation of the in-plane cyclic test of a RC bare frame conducted by Calvi and Bolognini (1999)

The RC bare frame that has been taken as reference has been tested by Calvi and Bolognini (1999) within an extensive experimental campaign on different weak clay masonry infills in RC frame. The specimens (full scale, one-storey, one-bay) were designed according to modern seismic codes as part of a new building and subjected to in-plane and out-of-plane tests. The testing procedure consisted in applying a constant load of 400 kN at the top of each column to simulate the presence of upper storeys and in imposing a gradually increasing cyclic horizontal displacement to the beam in order to perform a cyclic pseudo-static in-plane test up to 3.6% drift for the bare frame. The dimensions and the reinforcement of the RC frame are reported in Figures 6a and 6b, whereas the Force-Displacement experimental curve of the bare frame and application points of the loads are shown in Figure 6c.

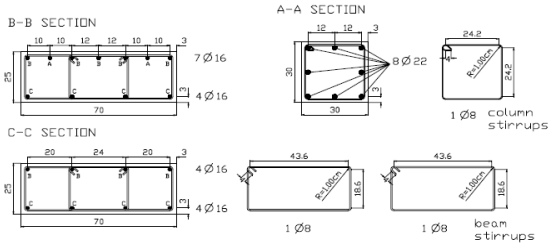

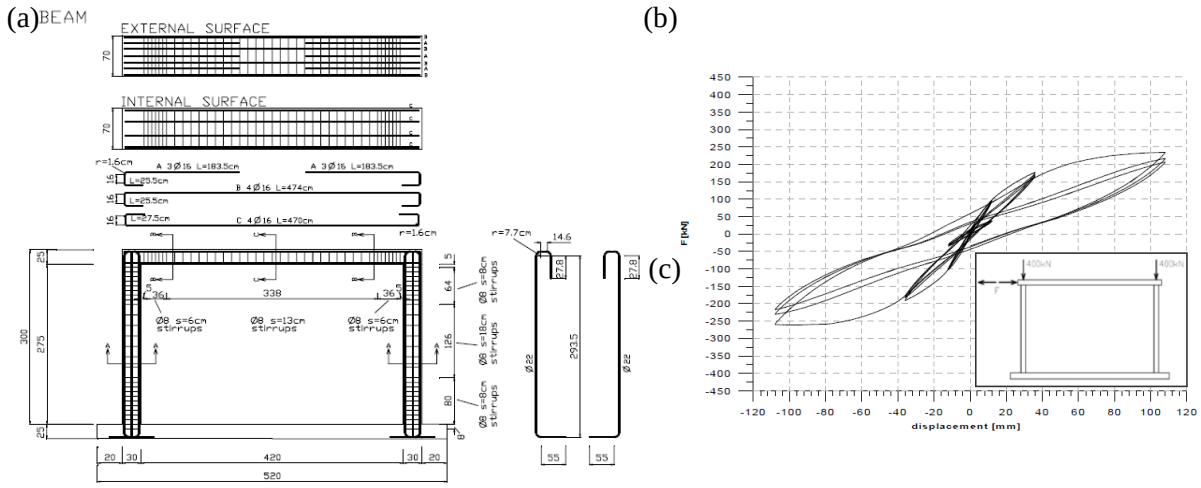

Figure 6. (a) Dimensions and reinforcement of the RC frame; (b) Detail of the sections of the RC frame; (c) Force-Displacement experimental curve of the bare frame and application points of the loads during the tests (Calvi and Bolognini, 1999).

As in the experimental testing campaigns, also the in the numerical studies is extremely important to have reliable results of the bare frame structure; indeed, as presented in *Section 5*, a comparison between the in-plane seismic performance of bare frame respect of the infilled frame allows a detailed interpretation of the results on the influence of the infill on the structure.

A phased analysis has been performed to replicate the experimental testing procedure; firstly the vertical loads were applied, secondly an incremental imposed displacement was imposed (pushover analysis). Four materials have been used according to the tests of characterization on the materials: the concrete of the beam, the concrete of the column, the steel of the longitudinal reinforcement and the steel of the transversal reinforcement. According to the reinforcement details, a clear cover of the concrete elements equal to 27 mm has been used. Only some of the experimental data on the mechanical characteristics of the concrete were available and, therefore, some values have been assumed making reference to the Eurocode 2 (CEN, 2004) and the CEB FIP 2010 Model Code (CEB/FIP, 2010). The properties of the concrete and of the reinforcement steel used in the FEM model are reported in more detail by Milanesi et al. (2015).

As shown in Figure 7a, the pushover analysis conducted on FEM has been able to predict the overall response of the bare frame; indeed, the numerical peak strength (225.5 kN) and the post-yield behaviour are really similar to the experimental results, where a peak strength of 227.7 kN has been obtained. Moreover, through the assumption of a Young modulus of the concrete equal to the 80% of the average elastic modulus evaluated with the expression in the EC2, the model has been able to match also the initial stiffness of the structure. The approximation of the Young modulus can be considered in line with the common dispersion of the values of this parameter. Figure 7b reports the deformed shape at the last drift obtained from the numerical simulation (4.3% drift).

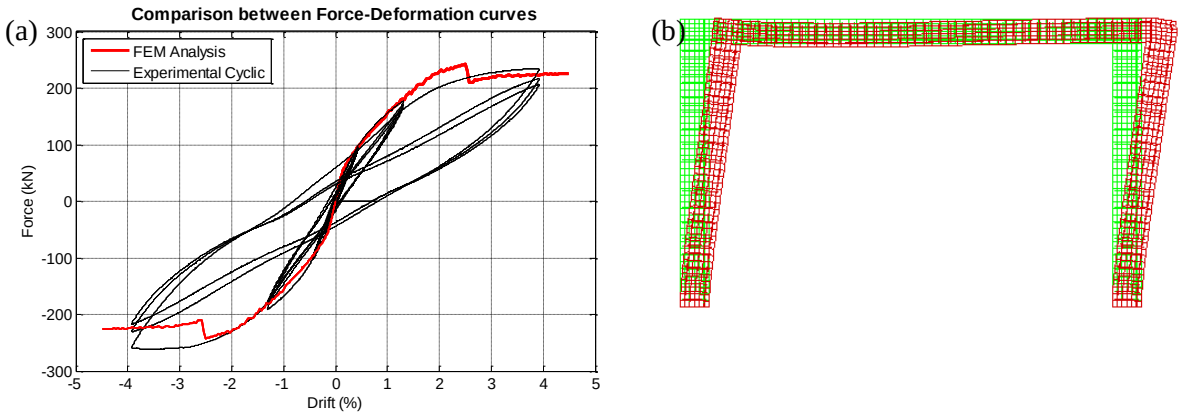

Figure 7. (a) Comparison Force-Displacement curves: pushover FEM analysis versus experimental cyclic results. (b) Deformed shape at 4.3% drift.

4.2 Numerical simulation of the in-plane cyclic test of a RC frame infilled with AAC URM conducted by Penna and Calvi (2006)

In 2006, several tests on AAC masonry infills have been conducted by Penna and Calvi (2006), using the same RC frames of the research by Calvi and Bolognini (1999). The experimental campaign has studied the seismic behaviour of different AAC infills: unreinforced, reinforced with a RC mid-height beam, reinforced with steel bars in the bed joints and a solution with a central opening. For the sake of this study, only the in-plane test on the AAC URM infill rigidly attached to the RC frame has been taken into account.

The specimen considered has tested up to a in-plane drift of 1.2%, in Figure 8a the cracking pattern at end of the test is reported, whereas the Force-Drift experimental curve is shown in black line in Figure 8b.

The same phased FEM analysis conducted for the bare frame model and described in *Section 4.1* has been carried out. The materials properties of the concrete and of the steel reinforcement assumed for the bare frame have been used for the infilled model. The properties of the AAC masonry have been calibrated as reported in *Section 3.2*. Moreover, an interface material has been included and modelled between the RC elements and the masonry. Further detail on values adopted and the modelling are reported in Milanesi et al. (2015).

Figure 8b, where the comparison between the Force-Drift experimental and numerical curves is reported, shows that the results of the FEM analysis are able to predict fairly well the overall behaviour of the structure.

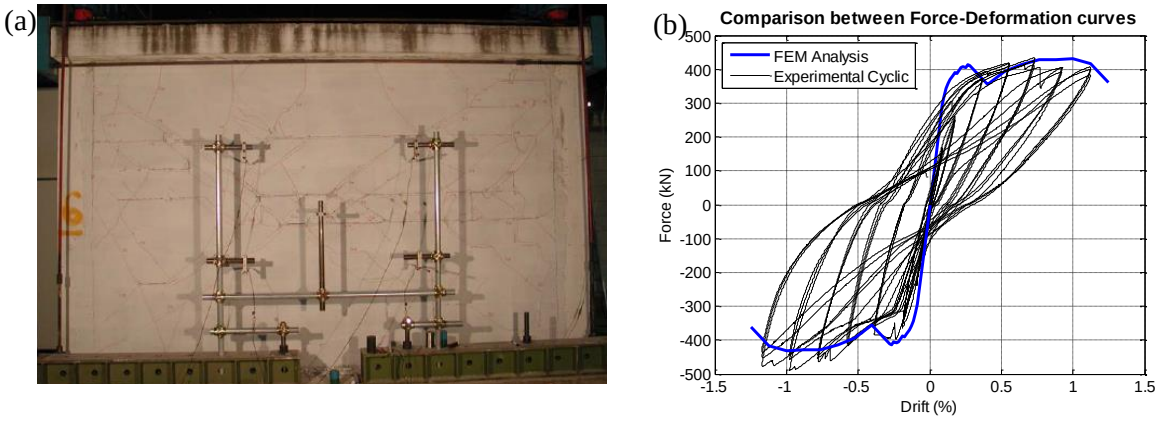

Figure 8. (a) Unreinforced AAC infill. (a) Crack pattern, (b) Comparison of the Force-Drift curves: experimental vs numerical.

The influence on the global seismic behaviour of the structure due to the infills is scientifically

recognised. Indeed, the variation of the deformed shape between the bare and the infilled frames is significant (Figure 9) and, for the AAC URM infilled RC frame studied, it dramatically changes depending from the drift. Furthermore, also the variation of the subdivision of the applied force into the base shear absorbed by the infill and taken by each RC column is altered due to the presence of the infill and it varies with the drift (Figure 10).

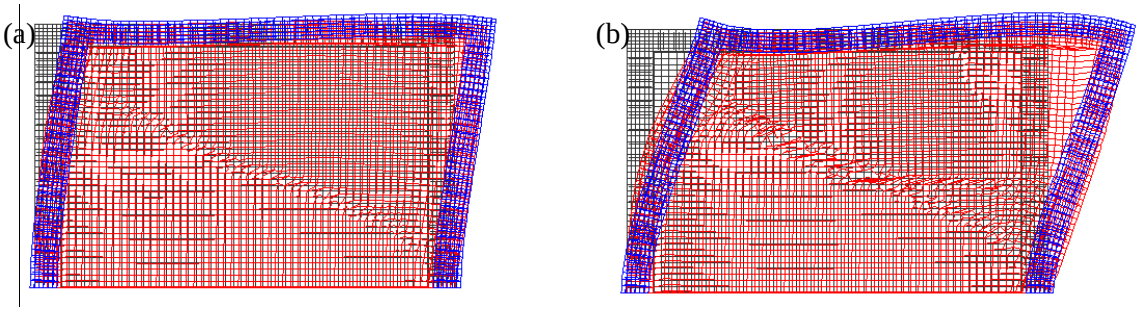

Figure 9. Comparison of the deformed shape of the RC bare frame (blue) and the infilled RC frame (red) at different drifts: (a) drift 0.50%, (b) drift 1.20%.

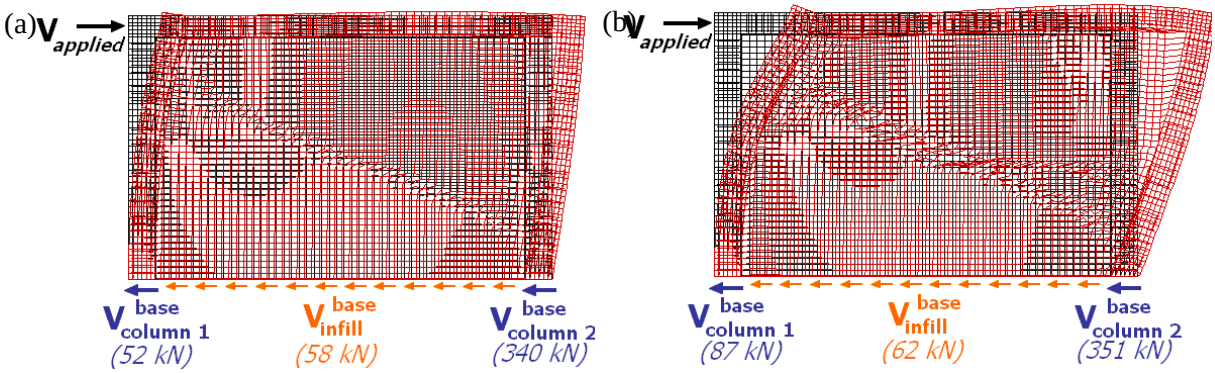

Figure 10. Base shear subdivision among RC columns and infill at: (a) drift 0.50%, (b) drift 1.20%.

5. LOCAL EFFECTS ON THE RC COLUMNS DUE TO THE INFILL

The post seismic surveys, even after earthquakes occurred recently, proved the possibility of occurrence of local effects on structural elements of infilled RC frame structures. In particular, the local damage and the brittle failure can interest RC columns in partial contact with infill. Indeed, the masonry panel causes a reduction of the clear height of the column and induces a local increase of the shear and displacement demands. Moreover, masonry infill typologies with high strength and stiffness has more probability to provoke detrimental local effects on RC columns of frame structures, especially if the infill is located only on one side of the column. In particular, additional concentrated shear demands may occur to the column edges, where there is the creation of a region of contact with the masonry infill due to the activation of the compressive diagonal strut, and possibly causing local column damage or shear failure.

The bending moment (Figure 11) and the shear demands (Figure 12) on the two RC columns of the bare frame show an almost symmetrical behaviour. They have been both calculated from the pushover analysis as a function of the imposed drift. Similarly, the moment and shear demand in case of AAC URM infilled frame are reported in Figure 12 and 13, respectively.

According to Table 1, there are evident differences between the bare and the infilled frames in terms of intensity and distribution of the internal forces. The changes start from the early low levels of imposed drift demand. The column of the infilled frame present a shear demand that is found to be almost constant up to the point where the local pressure of the infill begins to be activated and then it increases almost linearly up to the column edges; the maximum shear on the RC columns is always much larger than the one of the bare frame. Although also the moment distribution in the column of the infilled frame is very

different from the one of the bare frame, the maximum values are included between the maximum positive and negative moment of the bare structure. A comparison between the moment and shear demand at 0.3%, 0.5% and 1.0% is reported in Table 1.

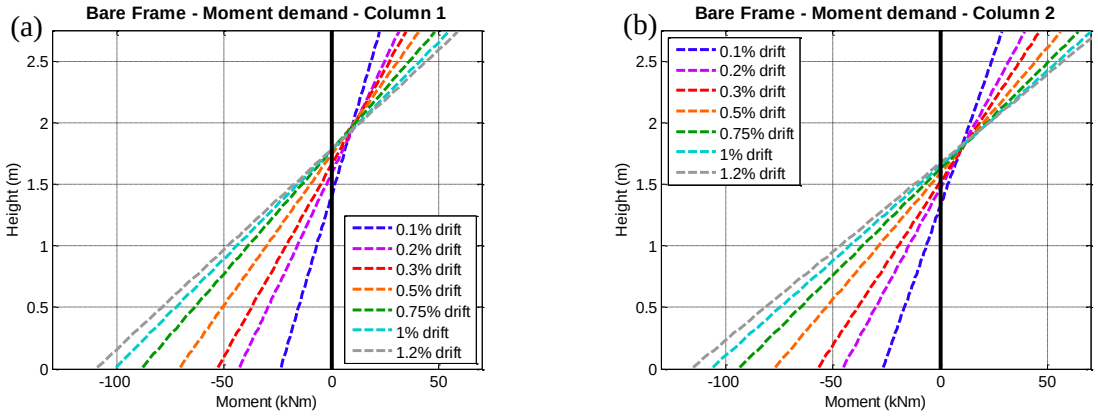

Figure 11. RC bare frame moment demand at different drifts (a) Column 1 (left), (b) Column 2 (right).

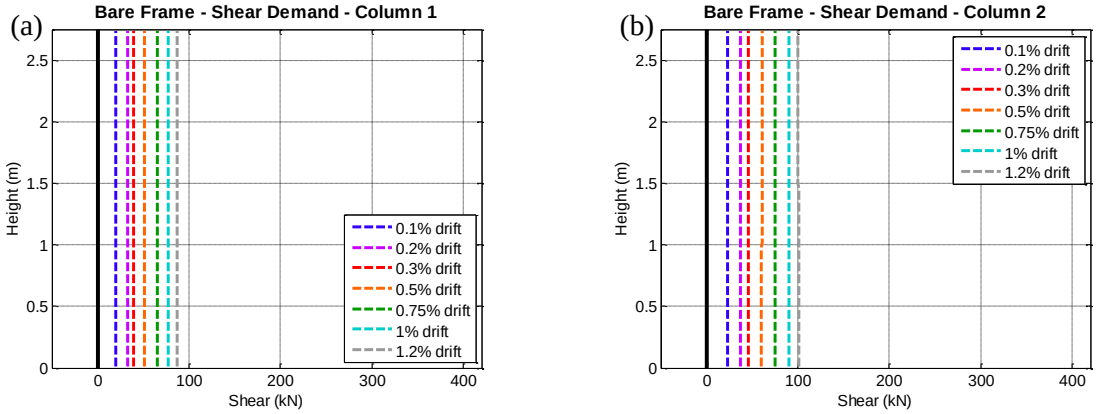

Figure 12. RC bare frame shear demand at different drifts (a) Column 1 (left), (b) Column 2 (right).

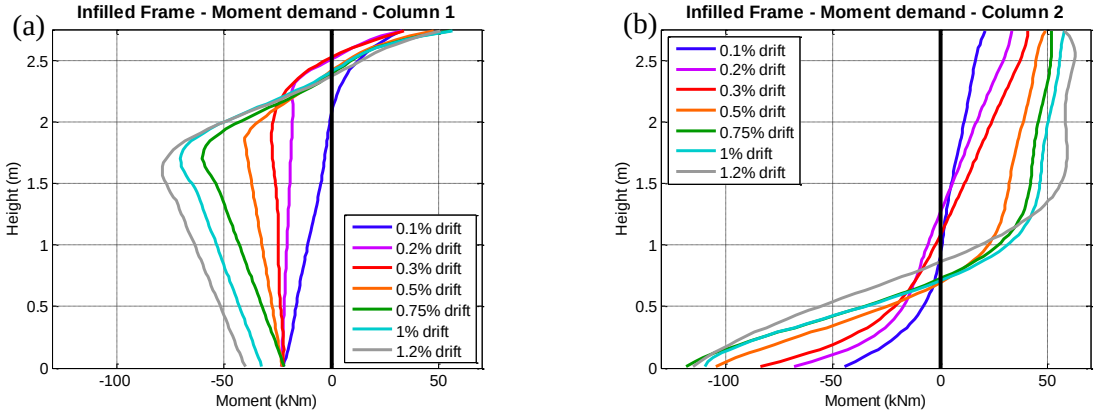

Figure 13. AAC infilled RC frame moment demand at different drifts (a) Column 1 (left), (b) Column 2 (right).

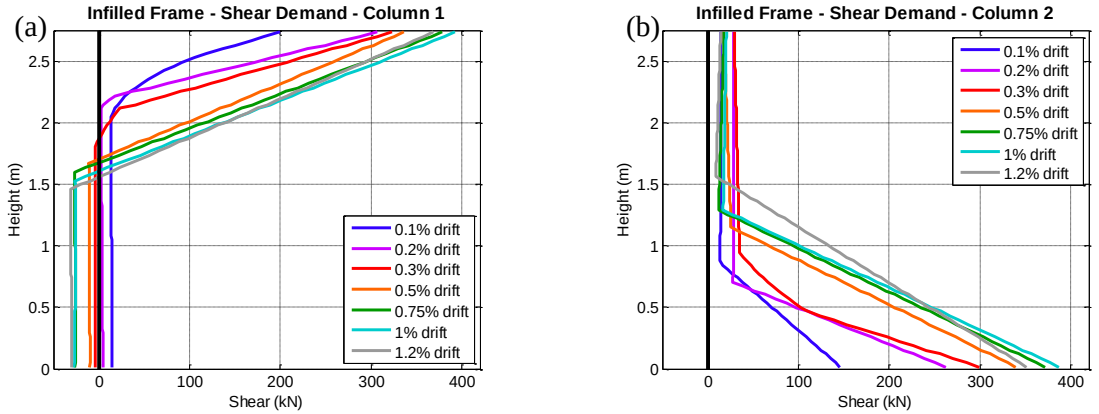

Figure 14. AAC infilled RC frame shear demand at different drifts (a) Column 1 (left), (b) Column 2 (right).

	Moment demand comparison	Shear demand comparison
Drift 0.3%	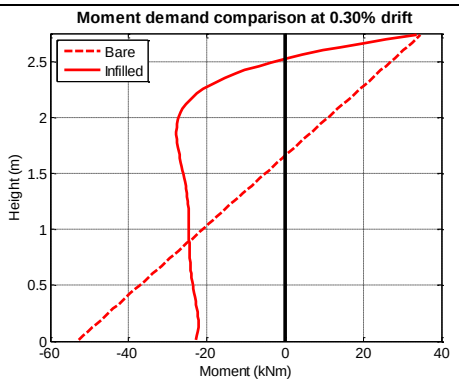	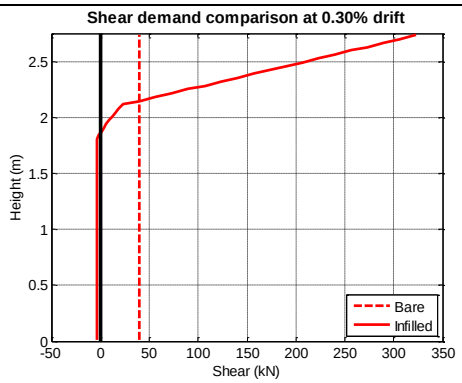
Drift 0.5%	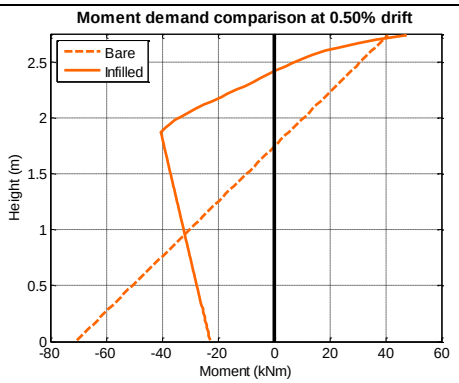	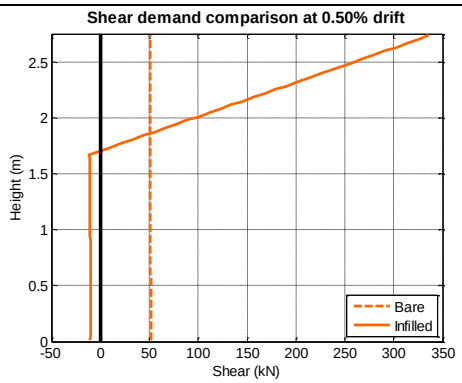
Drift 1.0%	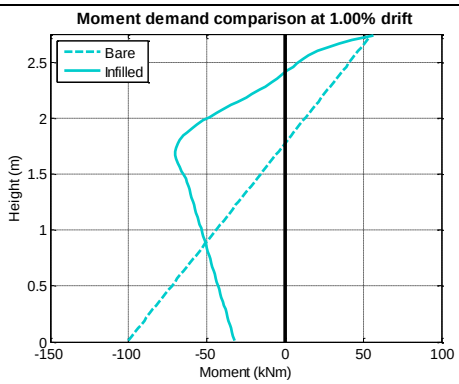	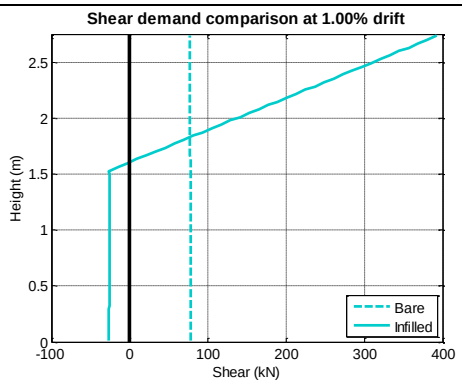

Table 1. Comparison of the moment and shear demand on RC column 1 of the RC bare frame and the AAC infilled RC frame at different drifts.

Furthermore, from the plots reported in Table 1 and Figure 15 a change of the shear demand depending from the applied displacement is clearly appreciable. The results are in agreement with the findings of other researchers with different masonry typologies (Buonopane et al., 1999; Bolis et al., 2017).
The local pressure distributions along the height of the column at different drifts for both column is shown in Figure 15, where the horizontal axis reports the dimensionless ratio between the stresses and the compressive strength of the masonry. The local pressure distribution shows a behaviour which is similar to a rectangular "stress block" from a drift of approximately 0.5%. Although the pressure distribution is dependent from the infill typology, the mechanical characteristics of the masonry, the interface material and other parameters, the local pressure distribution, for similar infill and masonry, is expected to increase (or decrease) proportionally with the mechanical characteristic of the masonry; thus, the shear demand and the local pressure may also be more detrimental than the results reported in Table 1 and Figures 15 and 16.

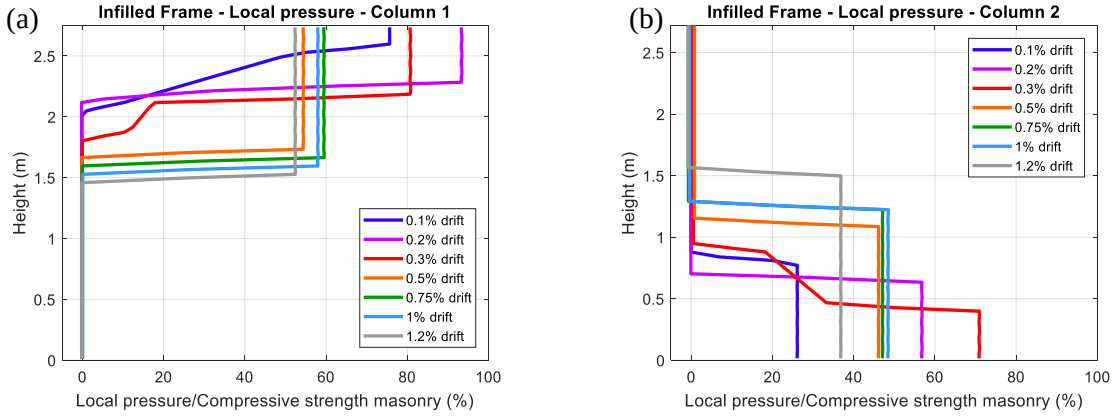

Figure 15. AAC infilled RC frame shear demand at different drifts (a) Column 1 (left), (b) Column 2 (right).

6. CONCLUSIONS

In the present work, a numerical simulation of in-plane tests conducted by Calvi and Bolognini (1999) and by Penna and Calvi (2006), for bare and AAC URM infilled frames, respectively, has been performed, and the local infill-frame interactions have been discussed.
In the non-linear static analyses performed using a FEM meso-model approach, the masonry of the infill has been calibrated according to tests of characterization. The numerical results of both the bare and infilled frames present a good matching with the Force-Displacement experimental curves and the cracking pattern observed during the tests.
The numerical simulation of the tests has allowed to obtain the actual moment and shear demand for each column at every imposed drift Thus, a comparison between the bare and the infilled frame has permitted to highlight the significant difference in the distribution of the internal forces in the case of AAC rigidly attached infill in comparison with the bare frame. The presence of the infill produces additional shear demand along the contact length and these local effects are relevant even at low levels of in-plane drift. The additional shear demand originates a local pressure that results in an almost rectangular stress block shape starting from 0.5% drift, when a complete activation of the diagonal strut occurred and evident damage in the masonry was observed.
Finally, this study on the local effects due to infill/RC frame interaction clearly needs further work including, for example, an investigation on the contact length variation in comparison with the imposed drift, a comparison of the numerical results with the approaches in literature, and an parametric application on a wider variety of masonry infills.

ACKNOWLEDGMENTS

The research, upon which this work is based, has been carried out at the University of Pavia/EUCENTRE and at the Middle East Technical University, and it has been sponsored by the

Erasmus Mundus Programme and by the Executive Projects DPC-RELUIS 2013-2016 and DPC-RELUIS 2017. The financial support for this study is gratefully acknowledged.

REFERENCES

Asteris PG, Kakaletsis DJ, Chrysostomou CZ, Smyrou E, (2011). Failure modes of infilled frames. *Electronic Journal of Structural Engineering*, **11**(1), 11-20.

Barzegar F, Maddipudi S, (1994). Generating reinforcement in FE modeling of concrete structures. *Journal of Structural Engineering*, **120**(5), 1656-1662.

Bolis V, Stavridis A, Preti M, (2017). Numerical investigation of the in-plane performance of masonry-infilled RC frames with sliding subpanels. *Journal of Structural Engineering*, **143**(2): 04016168.

Buonopane SG, White RN, (1999). Pseudo-dynamic testing of masonry infilled reinforced concrete frame. *Journal of Structural Engineering*, **125**(6), 578-589.

CEB/FIP (2010). Model Code 2010.

CEN (2004a). Eurocode 2 - Design of concrete structures, , Part 1-1: General rules and rules for building. Brussels, Belgium, *European Committee for Standardisation*, Part 1.1: General rules and rules for building.

CEN (2004b). Eurocode 8 - Design of structures for earthquake resistance, Part 1: General rules, seismic actions and rules for building. Brussels, Belgium, *European Committee for Standardisation*.

Calvi GM, Bolognini D, (1999). Seismic response of reinforced concrete frames infilled with weakly reinforced masonry panels. *Journal of Earthquake Engineering*, **5**, 153-185.

Da Porto F, Guidi G, Dalla Benetta M, Verlato N, (2012). Sistemi costruttivi e risultati sperimentali Reluis Research Report [in Italian]. *Experimental Report*, University of Padova, Italy.

EN (2001). UNI EN 1052-1 - Methods of test for masonry, Part 1: Determination of compressive strength. Brussels, Belgium, *European Committee for Standardisation*.

EN (2007). UNI EN 1052-3 - Methods of test for masonry, Part 3: Determination of initial shear strength. Brussels, Belgium, *European Committee for Standardisation*.

Fragomeli A., Galasco A., Graziotti F., Guerrini G., Kallioras S., Magenes G., Malomo D., Mandirola M., Manzini C.F., Marchesi B., Milanesi R.R., Morandi P., Penna A., Rossi A., Rosti A., Rota M., Senaldi I., Tomassetti U., Cattari S., da Porto F., Sorrentino L. (2017). Comportamento degli edifici in muratura nella sequenza sismica dell'Italia centrale del 2016 - Parte 1: Quadro generale [in Italian]. *Progettazione sismica* **8**(2), 49-77.

Hak S, Morandi P, Magenes G, (2013). Local effects in the seismic design of rc frame structures with masonry infill. *Proc. of 4th ECCOMAS COMPDYN*, 12-14 June, Kos Island, Greece.

Hordijk DA, (1991). Local Approach to Fatigue of Concrete. *PhD Thesis*, Delft, University of Technology, Netherland.

Lin, K., Totoev, Y.Z., Lin, H.J., (2011). In-plane cyclic test on framed dry-stack masonry panel. *Advanced Materials Research*, Vol. 163-167, pp. 3899-3903.

Lourenço PB, (1995). *An Orthotropic Continuum Model for the Analysis f Masonry Structures*. Delft, University of Technology, Netherland.

Manzini CF, Morandi P, (2012). Rapporto preliminare sulle prestazioni ed i danneggiamenti agli edifici in muratura portante moderni a seguito degli eventi sismici emilani del 2012 [in Italian]. **v.1**, Eucentre, *http://eqclearinghouse.org/2012-05-20-italy/*.

Markou G, Papadrakakis M, (2012). An efficient generation method of embedded reinforcement in hexahedral elements for reinforced concrete simulations. *Advances in Engineering Software*, **45**, 175-187.

Mehrabi AB, (1994). Behavior of masonry-infilled reinforced concrete frames subjected to lateral loading. *PhD Thesis*, University of Colorado, USA.

Milanesi R.R., Morandi P., Magenes G., Binici B., (2015). FEM simulation of the experimental response of AAC masonry infills in RC frames. *Proc. 5th ECCOMAS - COMPDYN 2015*, Crete, Greece, 25-27 May 2015.

Morandi P, Milanesi RR, Magenes G, (2016). Innovative seismic solution for clay masonry infills with sliding joints: principles and details. *Proc. of 16th IBMAC*, 26-30 June 2016, Padova, Italy.

Morandi, P., Hak, S., Magenes, G., (2017) “Performance-based interpretation of in-plane cyclic tests on RC frames with strong masonry infills”, Engineering Structures. Volume 156, 1 February 2018, Pages 503–521. https://doi.org/10.1016/j.engstruct.2017.11.058.

Penna A, Calvi GM, (2006). Campagna sperimentale su telai in c.a. con tamponamenti in Gasbeton (AAC) con diverse soluzioni di rinforzo [in Italian]. *Experimental Report, University of Pavia*, Italy.

Preti M, Bettini N, Plizzari G, (2012). Infill Walls with Sliding Joints to Limit Infill-Frame Seismic Interaction: Large-Scale Experimental Test. *Journal of Earthquake Engineering*, **16**(1), 125-141.

Roots JG, (1988). Computational modeling of concrete fracture. *PhD Thesis*, Delft, University of Technology, Netherland.

Selby RG, Vecchio FJ, (1993). Three-dimensional Constitutive Relations for Reinforced Concrete. *Technical Report 93-02*, University of Toronto, Toronto, Canada.

Stavridis A, (2009). Analytical and Experimental Study of Seismic Performance of Reinforced Concrete Frames Infilled with Masonry Walls. *PhD Thesis*, University of California, USA.

Tarque N, Candido L, Camata G, Spacone E, (2015). Masonry infilled frame structures: state of the art and review of numerical modeling. *Earthquakes and Structures*, **8**(1).

TNO-Diana, (2010). User's Manual - Version 9.4.3. Delft, Netherland.

Vecchio FJ, Collins MP, (1986). The Modified Compression-Field Theory for Reinforced Concrete Elements Subjected to Shear. *ACI Structural Journal*, **83**, 219-231.

Verlato N, Guidi G, Da Porto F, Modena C, (2016). Innovative systems for masonry infill walls based on the use of deformable joints: Combined in-plane/out-of-plane tests. *Proc. of 16th IBMAC*, 26-30 June 2016, Padova, Italy.

Vintzileou E, Adami CE, Palieraki V, (2016). In-plane and out-of-plane response of a masonry infilled divided into smaller wallettes. *Proc. of 16th IBMAC*, 26-30 June 2016, Padova, Italy.